Geophysical Research Letters

RESEARCH LETTER
10.1029/2021GL097222

Quantification of Seasonal and Interannual Variations of the Tibetan Plateau Surface Thermodynamic Forcing Based on the Potential Vorticity

Bian He[1,2], Chen Sheng[1,2], Guoxiong Wu[1,2], Yimin Liu[1,2], and Yiqiong Tang[1,3]

[1]State Key Laboratory of Numerical Modeling for Atmospheric Sciences and Geophysical Fluid Dynamics (LASG), Institute of Atmospheric Physics (IAP), Chinese Academy of Sciences, Beijing, China, [2]University of Chinese Academy of Sciences, Beijing, China, [3]Nanjing University of Information Science and Technology, Nanjing, China

Key Points:

- The Tibetan Plateau surface potential vorticity index (TP-SPVI) includes the effects from orographic thermal and dynamical forcing
- The seasonal variation in the proposed TP-SPVI is consistent with the time evolution of the Asian summer monsoon precipitation
- The surface PV can be used as a metric for the identification of the TP surface forcing in reanalysis data and for model evaluation

Supporting Information:

Supporting Information may be found in the online version of this article.

Correspondence to:

G. Wu and Y. Liu,
gxwu@lasg.iap.ac.cn;
lym@lasg.iap.ac.cn

Citation:

He, B., Sheng, C., Wu, G., Liu, Y., & Tang, Y. (2022). Quantification of seasonal and interannual variations of the Tibetan Plateau surface thermodynamic forcing based on the potential vorticity. *Geophysical Research Letters*, *49*, e2021GL097222. https://doi.org/10.1029/2021GL097222

Received 26 NOV 2021
Accepted 27 FEB 2022

Abstract In this study, a new index based on the potential vorticity (PV) framework is proposed for the quantification of the Tibetan Plateau (TP) surface thermodynamic and dynamic forcing. The results show that the derived TP surface PV (SPV) includes the topographical effect, near-surface absolute vorticity, and land–air potential temperature differences. The climatological annual cycle of the SPV suggests that the TP transitions from a cooling to a heating source in April. The SPV reaches a maximum from June to August, which is consistent with the evolution of the Asian summer monsoon precipitation. Further analysis suggests that the intensified SPV in the boreal summer results in a low-level cyclonic circulation anomaly associated with increased precipitation over the southeastern slope of the TP and South China and decreased precipitation over the Indian Ocean. In winter, the intensified SPV is associated with local cold air and divergence at the TP surface.

Plain Language Summary The thermal forcing of Tibetan Plateau (TP) has long thought to be important in regulating the Asian summer monsoon. However, the surface sensible heat flux cannot represent the total thermodynamic forcing of the TP because the SSHF decreases when the monsoon precipitation intensifies during the prevailing Asian summer monsoon season. In this study, we propose a new index based on the potential vorticity (PV) framework, which can be used to quantify seasonal and interannual variations in the TP's surface thermodynamic and dynamic forcing. The results show that the proposed index can represent the TP surface-elevated heating effect during the boreal summer, which is consistent with those of numerical experiments performed in previous studies. The new index can be used as a metric for model evaluation and climate characterization in future studies to quantify the role of the TP in global climate change.

1. Introduction

The climatic effects of the Tibetan Plateau (TP) have been intensively studied since the mid-twentieth century. Here TP is referred to not only its platform, but also the imbedded major mountain ranges including the Kunlun, the Gangdises, and the Himalayas. Traditionally, the thermal effects of the TP are considered to be the main driving forces for the generation of a circulation structure over the TP during the boreal summer (Chen & Trenberth, 1988; Duan & Wu, 2005; Flohn, 1957; Hoskins & Karoly, 1981; Hsu & Liu, 2003; Liu et al., 2007; Wu et al., 1997, 2015; Wu & Zhang, 1998; Ye et al., 1957; Ye & Gao, 1979), while the dynamical effect is also recognized as an important forcing in the formation of Asian climate (Bolin, 1950; Charney & Eliassen, 1949; Chiang et al., 2015, 2017, 2020; Liu et al., 2007; Queney, 1948; Son et al., 2019, 2020, 2021; Yeh, 1950). Theoretical and modeling studies have demonstrated that the relative importance of thermal forcing and mechanical forcing is very sensitive to the strength of the basic flow impinging upon the mountain (Held, 1983; Held & Ting, 1990; Held et al., 2002). The surface sensible heating is recognized as a crucial process based on which the TP surface thermal forcing drives atmospheric circulation, especially the heating on the southern slope of the TP (Wu et al., 2007).

The surface sensible heat flux (SSHF) over the TP has been calculated in many studies to identify the thermal forcing of the TP and its relationships with other climate systems (Duan et al., 2011, 2013, 2018; Han et al., 2017; Liu et al., 2020; Luo & Yanai, 1984; Ma et al., 2006, 2011; Wang et al., 2014; Yanai et al., 1992; Yang et al., 2009; Zhang & Wu, 1999; Zhao & Chen, 2000; Zhu et al., 2012; Y. Zhang et al., 2015; H. Zhang et al., 2019). However, the relationship between the summer SSHF over the TP and the Asian summer monsoon has been questioned

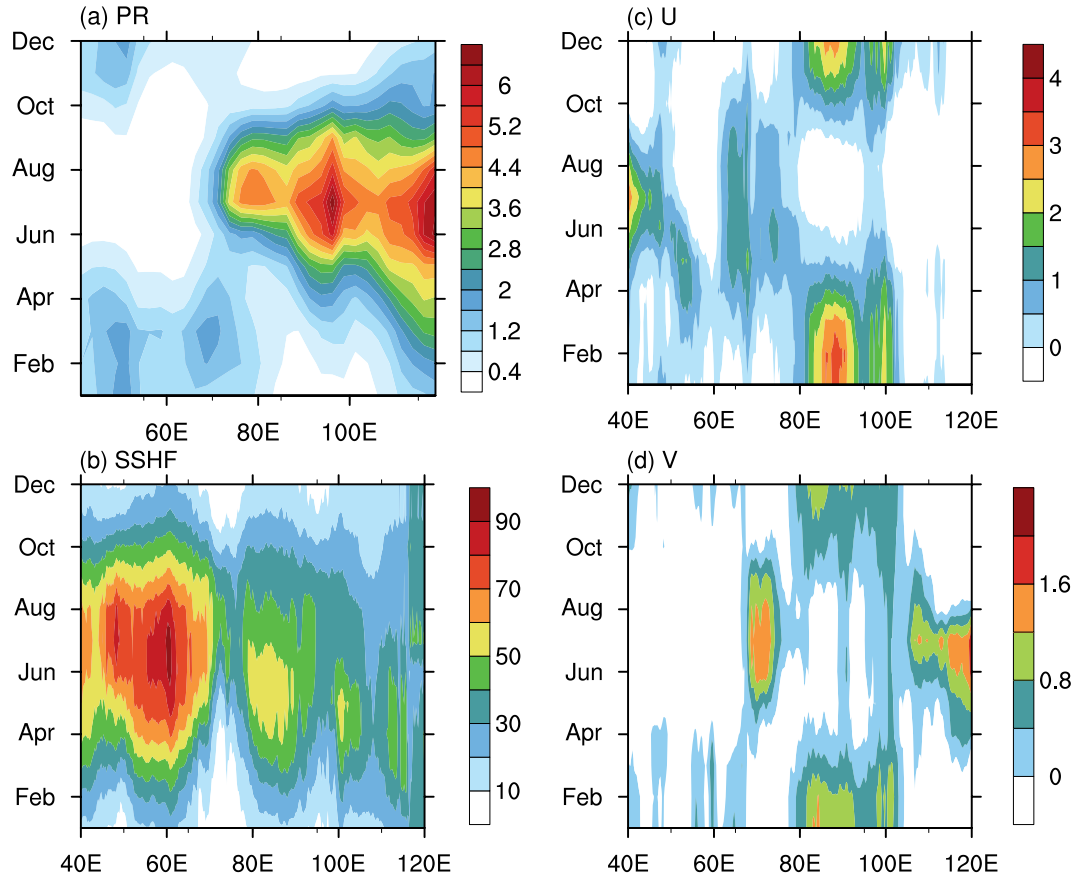

Figure 1. Climatological (1979–2019) annual cycle (25°–40°N mean) of the (a) precipitation (mm day^{-1}) from the Global Precipitation Climatology Project, (b) surface sensible heating flux (W m^{-2}) at an elevation above 500 m, (c) near-surface zonal wind (m s^{-1}), and (d) meridional wind (m s^{-1}) from the ERA5 reanalysis.

in recent studies (Boos & Kuang, 2010, 2013; Molnar et al., 1993; Rajagopalan & Molnar, 2013). They found that the surface heating over the TP only correlates with summer monsoon rainfall in the early (May 20 to June 15) and late (September 1 to October 15) monsoon seasons and is insignificant during the main monsoon season (June 15 to August 31).

Therefore, more studies must be carried out to understand the correlation between the TP thermodynamic status and the Asian monsoon system, which is complex, highly nonlinear, and physically coupled. For example, the SSHF alone cannot represent the overall surface heating effect of the TP. In terms of seasonal variations in the Asian summer monsoon in the subtropical region (25°–40°N; Figure 1 and Figure S2 in Supporting Information S1, OSM), the mean precipitation in the monsoon season becomes stronger and two maxima appear (close to a longitude of 95° and 120°E, respectively) from mid-April to August over both the South and East Asian land (Figure 1a and Figure S2b in Supporting Information S1). The seasonal evolution of the precipitation is accompanied by weakened westerly wind south of the TP in early April (Figure 1c) and intensified meridional wind over East Asia from May to August. However, the SSHF (Figure 1b) over the Iranian Plateau (IP, ~45°−70°E) is strong (>60 W m^{-2}) from April to August. In the TP region, the SSHF reaches a maximum from April to early June and then decreases when the monsoon precipitation increases from June to August. Theoretically, the SSHF can be expressed as follows:

$$\mathrm{SSHF} = \rho C_p C_H u \left(T_g - T_a\right), \tag{1}$$

where ρ is the air density, C_p is the specific heat capacity at constant pressure, C_H is the bulk transfer coefficient for heat, u is the full wind speed near the surface, T_g is the ground temperature, and T_a is the air temperature near the surface. The variation in the SSHF can be determined based on the product of the wind and land–air

temperature differences. During prevailing monsoon periods, both the westerly (Figure 1c) and meridional winds over the TP are weak, whereas strong precipitation cools the surface and leads to a decrease in the land–air temperature difference. This explains the negative correlation between the SSHF and monsoon precipitation in midsummer, as identified by Rajagopalan and Molnar (2013) and Zhang et al. (2019).

Although it remains unclear if the SSHF and Asian monsoon correlate during the boreal summer, the vertical diffusion heating over the TP was separated from other physical processes in a series of numerical experiments (He, 2017; He et al., 2015, 2019; Wu et al., 2012). The results of these experiments revealed that the TP surface sensible heating, especially the heating over the southern TP, indeed drives the generation of low-level circulation and surface air pumping over the TP. It remains unclear how this type of TP surface forcing in reanalysis datasets can be depicted to determine the role of TP surface thermodynamic forcing in Asian monsoon dynamics. In this study, we propose a new index, which can be used to determine the TP surface thermodynamic forcing based on the potential vorticity (PV) framework. The paper is structured as follows: The datasets and methods used in this study are introduced in Section 2. The features of the surface PV (SPV), both globally and in the TP region, are described in Section 3. The constructed TP thermodynamic forcing index and its correlation with the Asian monsoon system are presented in Section 4. The conclusions and discussion are provided in Section 5.

2. Data Sets and Method

2.1. Data Sets

The ECMWF Reanalysis v5 (ERA5) data sets from the European Center for Medium-Range Weather Forecasts (ECMWF; Hersbach et al., 2020) were used to determine the multilevel air temperature, specific humidity, and wind field. The observed precipitation data were adopted from the Global Precipitation Climatology Project (GPCP) monthly mean data set (Adler et al., 2003). The study period was 1979–2019.

2.2. Method

The PV is a variable, which was proposed in the 1940s (Ertel, 1942; Rossby, 1940) and has been widely used for the analysis of synoptic events and climate change on isentropic surfaces (Aebischer & Schar, 1998; Haynes & McIntyre, 1987, 1990; Hoskins, 1991; Hoskins et al., 1985; Thorpe, 1985). In general, the three-dimensional PV can be expressed as:

$$PV = \alpha \vec{\xi_a} \cdot \nabla_3 \theta, \tag{2}$$

where α is specific volume, $\vec{\xi_a}$ is three-dimensional absolute vorticity, and θ is potential temperature. The PV of adiabatic and frictionless motions is conservative. Therefore, the changes in the PV can be used to identify processes related to diabatic heating and friction in a unified framework.

On Earth's surface, the application of traditional isentropic coordinates is not suitable because isentropic surfaces intersect with the surfaces of large mountainous areas. Therefore, a terrain-following coordinate model was adopted for the derivation of the SPV over orographic regions. We introduced the hydrostatic balance and σ coordinates:

$$\frac{\partial p}{\partial z} = -\rho g \tag{3}$$

and

$$\sigma = \frac{p}{ps}, \tag{4}$$

into Equation 2. In a recent study (Sheng et al., 2021), each term in the three-dimensional PV was analyzed for different time scales. At seasonal mean time scales the vertical component product was identified to be the dominant term, whereas the horizontal component product was relatively small (see Figure S3 in Supporting Information S1). Therefore, for simplicity, we used the vertical component product of the PV in the terrain-following

coordinate model to estimate the TP surface thermodynamic forcing. The vertical PV product in the σ coordinate system can be simplified as follows:

$$\mathrm{PV}_{\sigma} = -\frac{g}{ps}\left(f + \zeta_{\sigma}\right)\frac{\partial\theta}{\partial\sigma}, \tag{5}$$

where ζ_{σ} denotes the relative vorticity in the σ coordinate system. On Earth's surface, Equation 5 can be expressed as:

$$\mathrm{PV}_{\sigma_1} = -\frac{g}{ps}\left(f + \zeta_{\sigma_1}\right)\frac{\theta_s - \theta_a}{1 - \sigma_1}, \tag{6}$$

where σ_1 denotes the first σ level above the Earth's surface, which is the bottom level of the atmospheric model; ζ_{σ_1} is the relative vorticity at the σ_1 level; θ_s is the potential temperature at the Earth's surface; and θ_a is the air potential temperature at the σ_1 level. The distribution and variability of PV_{σ_1} are mainly determined by the orographic effect ($\frac{1}{ps}$), surrounding circulation (ζ_{σ_1}), and vertical difference in the potential temperature ($\theta_s - \theta_a$), which is related to the vertical sensible heat flux. Therefore, the comparison of Equations 6 and 1 reveals that the vertical PV product is more suitable for the estimation of the surface forcing effect over the TP and adjacent regions than the SSHF. Because f is generally larger than ζ, the sign of PV_{σ_1} is determined by the land–air potential temperature difference ($\theta_s - \theta_a$) in the same hemisphere. In this study, we defined a new variable based on the SPV:

$$\mathrm{PV}^{*}_{\sigma_1} = -\mathrm{PV}_{\sigma_1} = -\left[-\frac{g}{ps}\left(f + \zeta_{\sigma_1}\right)\frac{\theta_s - \theta_a}{1 - \sigma_1}\right]. \tag{7}$$

Thus, $\mathrm{PV}^{*}_{\sigma_1}$ is positive/negative when the land–air potential temperature difference ($\theta_s - \theta_a$) is positive/negative, which is related to the positive/negative heating gained from the Earth's surface.

3. SPV Distribution in Reanalysis Data Sets

The seasonal and interannual variations in the SPV were analyzed. As noted in Section 2.2, the orographic elevation in terms of the surface pressure ($\frac{1}{ps}$), absolute vorticity ($f + \zeta_{\sigma_1}$), and vertical heating element ($\theta_s - \theta_a$) are the three key components that control the variation in distribution of the SPV. To understand the relative importance of these factors for the seasonal mean SPV, the global distributions of the SPV and the three components are shown in Figure 2. In general, the June, July, and August (JJA) SPV (Figure 2a) show positive values in the Northern Hemisphere and negative values in the Southern Hemisphere. The maximum SPV is located over the Tibetan and Iranian plateaus (TIPs) in Asia and the Rocky Mountains in North America. In December, January, and February (DJF; Figure 2e), the SPV exhibits strong negative values over the TIPs and Rocky Mountains, which contrasts the JJA pattern. The SPV shows two strong anomalies over the northwestern Pacific and northwestern Atlantic oceans. These findings are consistent with the concept proposed in pioneering studies (Ye et al., 1957; Ye & Gao, 1979) based on which the TP is a heat source in the boreal summer and cold source in the boreal winter and plays a dominant role in regulating climate change over East Asia. Thus, by analyzing Equation 7, the change in the SPV can be considered as a measurement for the change in the TP thermal and dynamic forcing.

Figures 2b and 2f show the vertical heating elements ($\theta_s - \theta_a$) in JJA and DJF, respectively. Over Asia and North America, the distributions of the vertical heating elements ($\theta_s - \theta_a$) are very similar to the total SPV in both seasons. These patterns suggest that the land–air heat exchange is the most important factor enabling large-scale mountains to drive atmospheric circulation. This exchange is also the dominant PV source at the surface. The absolute vorticity term ($f + \zeta_{\sigma_1}$) in JJA (Figure 2c) and DJF (Figure 2g) is similar. It is almost zonally symmetric at the global scale and increases with latitude. The absolute vorticity is negative in the Southern Hemisphere and positive in the Northern Hemisphere. This term can intensify the SPV at high latitudes in both hemispheres. The topographic elevation term is expressed as the reciprocal of the surface pressure and is shown in Figures 2d and 2h for JJA and DJF, respectively. This term has a unique maximum over the TP and is almost twice that of other non-elevated areas, which indicates that the orographic elevation term in Equation 7 can intensify the total SPV over the TP compared with other regions and that the TP is a PV source.

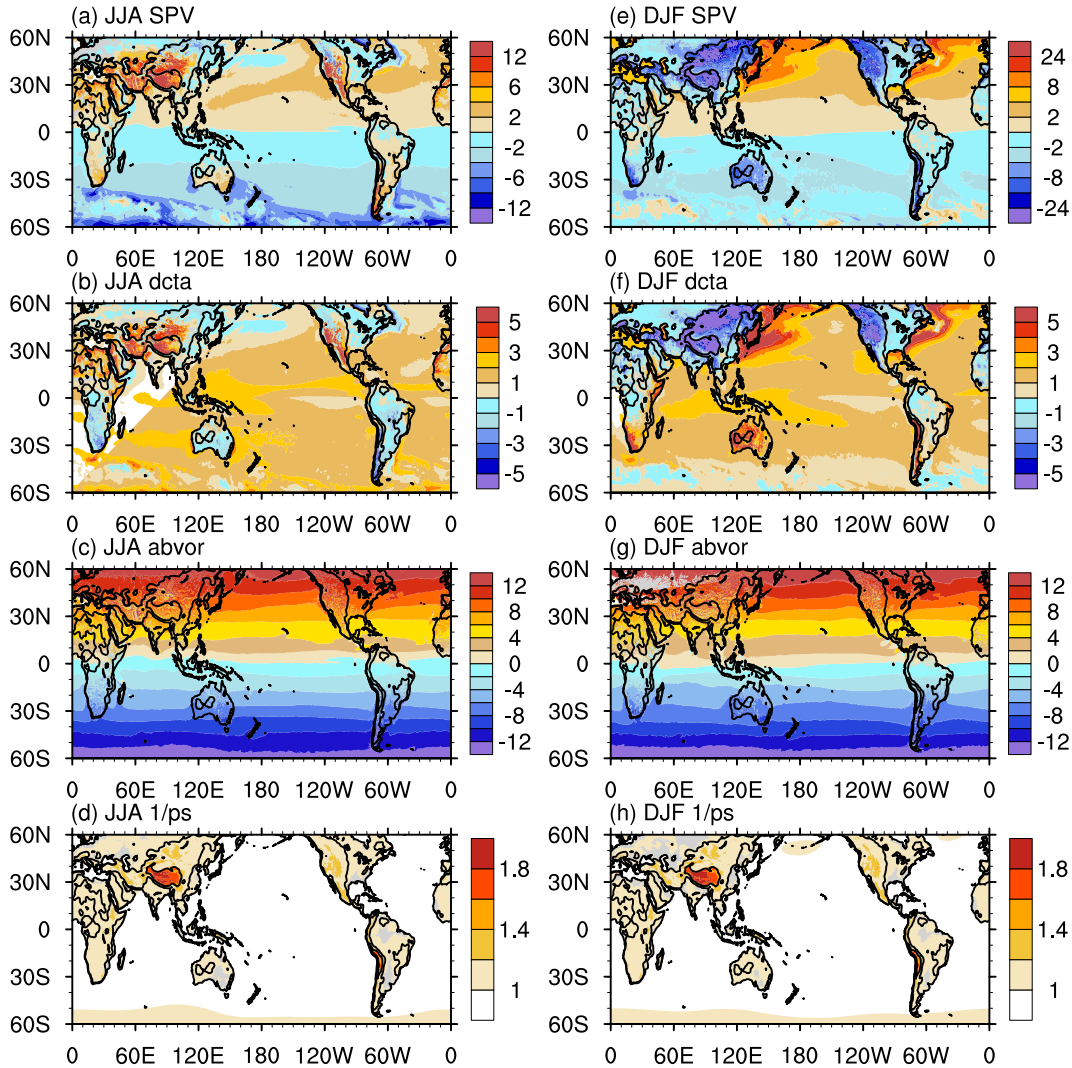

Figure 2. Climatological (1979–2019) spatial distribution of the SPV (PVU, 1PVU = 10^{-6} K m^2 kg^{-1} s^{-1}) in (a) JJA and (e) December, January, and February (DJF) based on the ERA5 reanalysis. Land–air potential temperature difference ($\theta_s - \theta_a$) (k) in (b) June, July, and August (JJA) and (f) DJF. Absolute vorticity ($f + \zeta_{\sigma_1}$; 10^{-5} s^{-1}) in (c) JJA and (g) DJF. Orographic elevation effect ($\frac{1}{ps}$; 10^{-3} hPa^{-1}) in (d) JJA and (h) DJF.

The above-mentioned analysis provides a basis for estimating the intensity of the orographic surface forcing by quantifying the SPV over the TP region. Below, we further discuss the climatological annual cycle of the SPV over the TP region (Figure 3) and compare it with the seasonal evolution of the SSHF and Asian monsoon system (Figure 1). The annual cycle of the mean SPV averaged over the 25°–40°N band (Figure 3) indicates that the TP (80°−100°E) changes from a negative PV source (cold source) to a positive PV source (heat source) from March to April. The SPV gradually intensifies and reaches its maximum from June to early August. Subsequently, it decreased from August to October and changed to a negative PV source again during late September, which is consistent with the seasonal evolution of the Asian summer monsoon precipitation (Figure 1 and Figure S2 in Supporting Information S1) and intensified meridional winds over East Asia from June to August (Figure 1d). The positive PV is associated with the bend of isentropic surface in the lower troposphere and leads to cyclonic anomaly. It can contribute to the East Asian land precipitation. It's interesting that the IP is also a strong PV source throughout the year, except from November to January. The SPV over the IP also reaches its maximum from June to August, but the intensity is weaker than that over the TP. This implies that the TP and IP jointly form an important topographic thermodynamic forcing that could affect the variations of the Asian summer monsoon, which agrees with the results of previous studies (He et al., 2015; Liu et al., 2017; Wu et al., 2012, 2016, 2017).

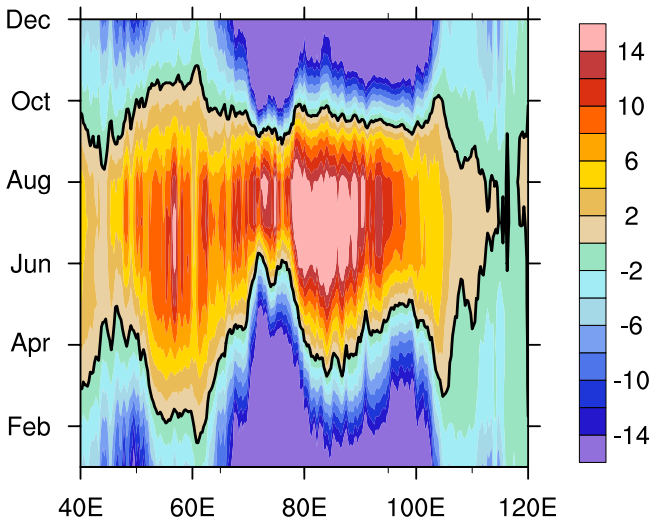

Figure 3. Climatological (1979–2014) annual cycle of the surface potential vorticity (SPV [PVU]) averaged over the (25°–40°N) zone with an elevation >500 m. The thick black line denotes the zero line of the SPV.

4. Index for the Measurement of the TP Thermodynamic Forcing Based on the SPV

The analysis of seasonal and interannual SPV characteristics in the previous section suggests that the SPV can accurately depict the changes in the TP thermodynamic forcing. In the terrain-following coordinate, the SPV along the TP surface becomes a horizontally integrated SPV along the σ surface. Thus, the calculation of the total SPV over the TP surface on the σ surface can be used to determine the integrated intensity of the TP thermodynamic forcing. Based on Equation 7, we defined an index for the estimation of the total TP surface thermodynamic forcing (TP-SPVI) on a σ surface:

$$I_{\mathrm{TP}} = \iint \mathrm{PV}^{*}_{\sigma_1} dxdy = \iint -\left[-\frac{g}{ps}\left(f+\zeta_{\sigma_1}\right)\frac{\theta_s-\theta_a}{1-\sigma_1}\right] dxdy. \quad (8)$$

In this study, the TP region we focus mainly covers the area ranging from 25° to 40°N and 70°−110°E, with an elevation above 500 m. It includes the southern boundary of the Himalayas and many large, interior mountain ranges. The evolution of the JJA mean I_{TP} from 1979 to 2019 is shown in Figure 4a. The JJA I_{TP} ranges from ~39.5 potential vorticity unit (PVU) km^2 to 55 PVU km^2 and exhibits an interannual variability. The long-term variation in TP thermal forcing increases from 1979 to 1998 and decreases from

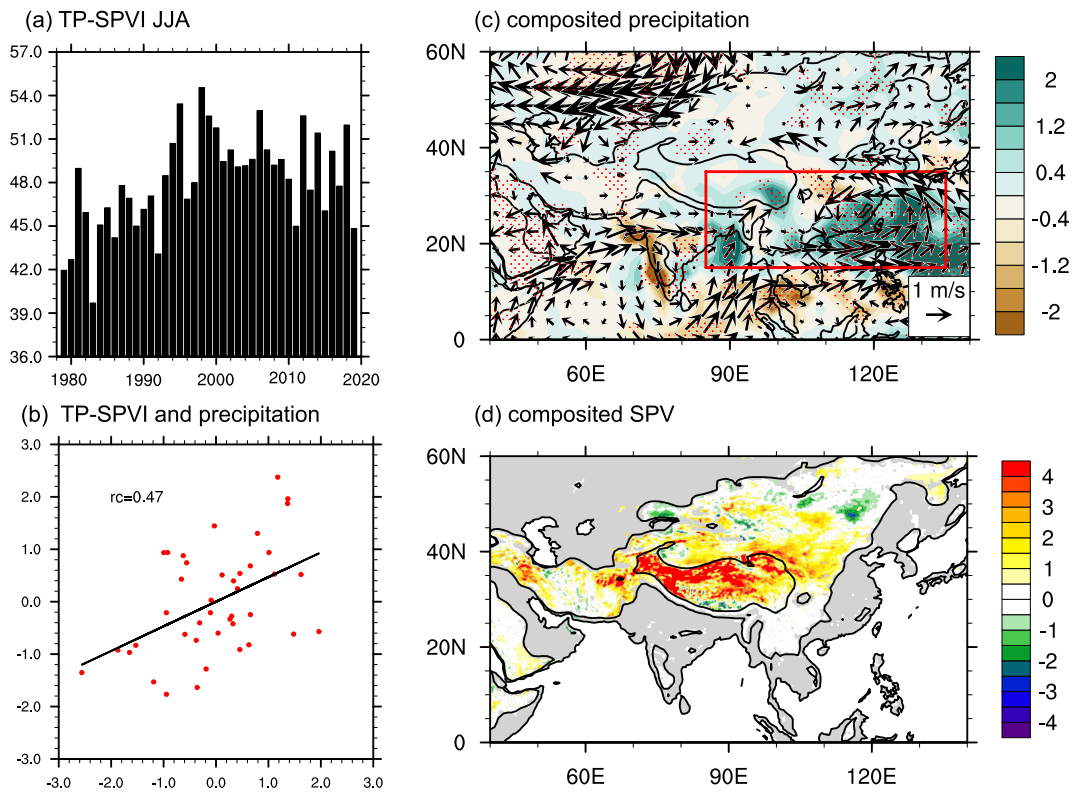

Figure 4. (a) Bar chart for the TP-SPVI from 1979 to 2019 (PVU km^2). (b) Linear fit between the standardized JJA TP-SPVI (horizontal axis) and regional mean (15°–35°N, 85°−135°E) precipitation (vertical axis). The regression coefficient is 0.47 (identical to the calculated Pearson correlation coefficient). (c) Composite differences in the JJA precipitation (mm day^{-1}) and winds (m s^{-1}) at 850 hPa. The red dots are statistically significant at the 99% confidence level based on a Student's *t*-test. (d) Composite difference of JJA SPV (PVU). The thick black contours denote the topographic heights of 3,000 and 500 m, respectively. The red rectangle denotes the area (15°–35°N, 85°−135°E).

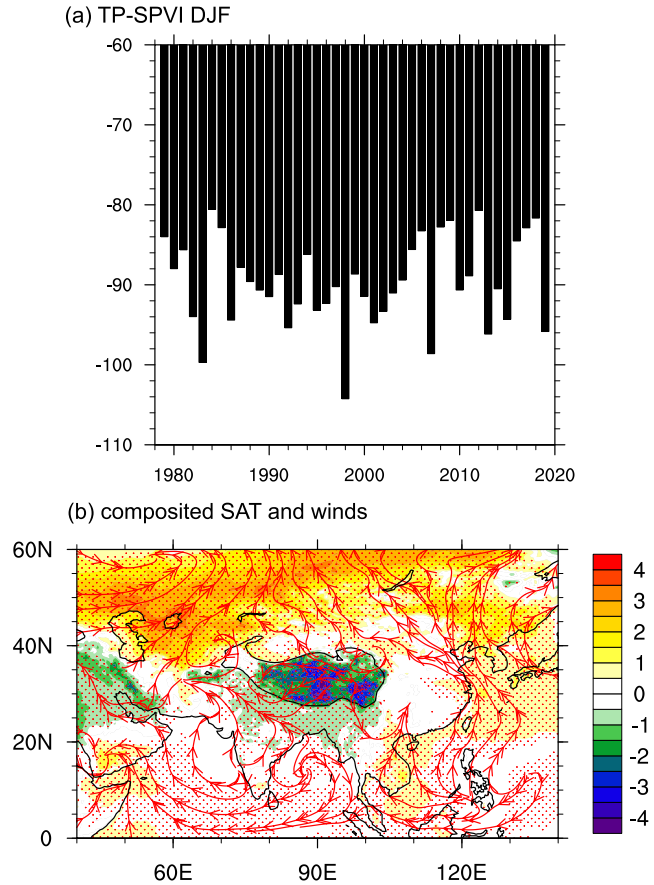

Figure 5. (a) Bar plots for the DJF mean TP-SPVI from 1979 to 2019 (PVU km^2). (b) Composite differences in the surface air temperature (°C) and surface streamlines for the winds. The dotted region indicates statistical significance at the 99% confidence level based on a Student's *t*-test. The thick black contour denotes a topographic height of 3,000 m.

1998 to 2019. Decomposition analysis indicates that the potential temperature term dominates this variation (Figure S4 in Supporting Information S1).

We further calculated the standard deviation of the I_{TP} and defined the strong/weak years based on the I_{TP} above/below the one-time standard deviation of the composite analysis. Among the 41 years, 7 years are strong (1995, 1998, 1999, 2000, 2006, 2012, and 2018) and 6 years are weak (1979, 1980, 1983, 1986, 1992, and 2019). To understand the corresponding monsoon circulation and precipitation changes associated with the I_{TP} intensity, we calculated the composites for the strong and weak years, respectively. The differences in the wind at 850 hPa and precipitation are shown in Figure 4c together with the associated changes in the SPV (Figure 4d). The SPV difference exhibits a positive pattern over the TP surface, with a maximum exceeding 4 PVU over the northwestern part of the TP (Figure 4d). The associated changes in the Asian summer monsoon circulation (Figure 4c) indicate a clear cyclonic pattern over the TP, with a positive precipitation difference over the southeastern edge of the TP and subtropical western Pacific. A negative precipitation difference can be mainly observed over the western part of India, the Indian Ocean, and the southern Indochina Peninsula. This pattern is very similar to the monsoon responses to the TP surface heat forcing derived from numerical simulations, as shown in Figure 3b of Wu et al. (2012) and Figure 2b of He et al. (2019). This result further confirms that our definition of the I_{TP} can capture the TP thermal forcing states during the boreal summer and the composite results are consistent with those of numerical experiments. Figure 4b shows the linear regressions and correlations between the standardized I_{TP} and regional mean precipitation averaged over the area (15°–35°N, 85°−135°E; Figure 4c). The regression coefficient was determined to be 0.47 (identical to the calculated Pearson correlation coefficient), implying that the intensified SPV over the TP can intensify the precipitation over the South and East Asian land.

Compared with the extensively studied effects of the TP thermodynamic forcing during the boreal summer, the effects of the TP thermodynamic forcing during the boreal winter have been rarely studied. To determine whether the new index proposed in this study is applicable to the boreal winter, we calculated the TP SPV and associated surface temperature and circulation. Figure 5a shows the evolution of the DJF mean I_{TP} values from 1979 to 2019. Based on the figure, the I_{TP} is negative in winter, suggesting that the TP is a cold source during the boreal winter, which agrees with previous results.

In addition, a composite analysis based on the one-time standard deviation of the I_{TP} was carried out to gain insights into the associated circulation and thermal structure related to the SPV changes in winter. The strong/weak years of the TP winter forcing are defined by the individual I_{TP} below or above one-time standard deviation. Among the 41 years, 7 years are strong (1983, 1992, 1998, 2001, 2007, 2013, and 2019) and 9 years are weak (1979, 1984, 1985, 2006, 2008, 2009, 2012, 2017, and 2018). The composite differences in the winter surface air temperature and near-surface winds at 10 m are shown in Figure 5b. The cooling of the TP during winter is associated with a surface divergence anomaly over the TP, based on which the surface air is advected to both the northern and southern TP. The air flow anomaly is accompanied by surface air temperature changes, that is, mainly cooling on the TP above 3,000 m, weak cooling over northern India, and warming over mid–high latitudes north of the TP. The above-mentioned analysis proves that the new scalar index represents the intensity of the surface temperature and wind anomaly over TP during the boreal winter. Finally, we also examined the composited precipitation associated with the changes in the SPV during the boreal winter (Figure S5 in Supporting Information S1). The SPV correlates with precipitation changes over South China land and maritime continents over Western Pacific; however, the mechanism requires further studies.

5. Conclusions and Discussions

The SSHF has been used for a long time to estimate the TP surface heating status. However, the SSHF only partially represents the TP surface thermal forcing because the correlation between the SSHF over the TP and Asian summer monsoon precipitation is unclear. In this study, we constructed a new variable SPV to measure the intensity of the TP thermodynamic forcing based on the PV framework. The SPV is mainly controlled by the near-surface vorticity, elevation, and potential temperature differences between the land and surface air associated with the SSHF. The annual cycle of the SPV suggests that the TP transitions from a cold source to a heat source, primarily in April, reaches its maximum from June to August, and transitions from a heat source to a cold source in late September, which is consistent with the development of the Asian monsoon system as well as previous results of numerical experiments of the effects of the TP surface heating. The above-mentioned analyses confirm that the SPV over the TP is representative of the mountain's thermodynamic as well as dynamic forcing and that the potential temperature difference term is dominant in the boreal summer. It can also be a measurement for the dynamical effect which may be important in different timescales. Therefore, the SPV can be used as a metric for model and climate evaluations to quantitatively estimate the role of the TP in global climate change.

Data Availability Statement

The ERA5 data set is available at https://www.ecmwf.int/en/forecasts/datasets/reanalysis-datasets/era5. The GPCP precipitation data set is available at http://www.esrl.noaa.gov/psd/data/gridded/data.gpcp.html.

Acknowledgments
The research presented in this paper is jointly funded by the National Natural Science Foundation of China (Grant Nos. 41730963, 91837101, 42122035, and 91937302), the National Key Research and development Program of China (Grant No. 2020YFA0608903), and the Guangdong Major Project of Basic and Applied Basic Research (2020B0301030004). The authors also thank the two anonymous reviewers for their constructive suggestions, which have improved the overall quality of the manuscript.

References

Adler, R. F., Huffman, G. J., Chang, A., Ferraro, R., Xie, P. P., Janowiak, J., et al. (2003). The version-2 global precipitation climatology project (GPCP) monthly precipitation analysis (1979–present). *Journal of Hydrometeorology*, *4*, 1147–1167. https://doi.org/10.1175/1525-7541(2003)004<1147:tvgpcp>2.0.co;2

Aebischer, U., & Schär, C. (1998). Low-level potential vorticity and cyclogenesis to the lee of the Alps. *Journal of the Atmospheric Sciences*, *55*, 1862–207. https://doi.org/10.1175/1520-0469(1998)0552.0.CO

Bolin, B. (1950). On the influence of the Earth's orography on the general character of the westerlies. *Tellus*, *2*, 184–195. https://doi.org/10.3402/tellusa.v2i3.8547

Boos, W. R., & Kuang, Z. (2010). Dominant control of the South Asian monsoon by orographic insulation versus plateau heating. *Nature*, *463*, 218–222. https://doi.org/10.1038/nature08707

Boos, W. R., & Kuang, Z. (2013). Sensitivity of the South Asian monsoon to elevated and non-elevated heating. *Scientific Reports*, *3*. https://doi.org/10.1038/srep01192

Charney, J. G., & Eliassen, A. (1949). A numerical method for predicting the perturbation of the middle latitude westerlies. *Tellus*, *1*, 38–54. https://doi.org/10.3402/tellusa.v1i2.8500

Chen, S. C., & Trenberth, K. E. (1988). Orographically forced planetary-waves in the Northern Hemisphere winter—Steady-state model with wave-coupled lower boundary formulation. *Journal of the Atmospheric Sciences*, *45*, 6572–681. https://doi.org/10.1175/1520-0469(1988)045<0657:ofpwit>2.0.co;2

Chiang, J. C. H., Fung, I. Y., Wu, C. H., Cai, Y. J., Edman, J. P., Liu, Y. W., et al. (2015). Role of seasonal transitions and westerly jets in East Asian paleoclimate. *Quaternary Science Reviews*, *108*, 111–129. https://doi.org/10.1016/j.quascirev.2014.11.009

Chiang, J. C. H., Kong, W., Battisti, D., & Battisti, D. S. (2020). Origins of East Asian summer monsoon seasonality. *Journal of Climate*, *33*, 7945–7965. https://doi.org/10.1175/jcli-d-19-0888.1

Chiang, J. C. H., Swenson, L., & Kong, W. (2017). Role of seasonal transitions and the westerlies in the interannual variability of the East Asian summer monsoon precipitation. *Geophysical Research Letters*, *44*, 3788–3795. https://doi.org/10.1002/2017gl072739

Duan, A. M., Li, F., Wang, M. R., & Wu, G. X. (2011). Persistent weakening trend in the spring sensible heat source over the Tibetan Plateau and its impact on the Asian summer monsoon. *Journal of Climate*, *24*, 5671–5682. https://doi.org/10.1175/jcli-d-11-00052.1

Duan, A. M., Liu, S. F., Zhao, Y., Gao, K. L., & Hu, W. T. (2018). Atmospheric heat source/sink dataset over the Tibetan Plateau based on satellite and routine meteorological observations. *Big Earth Data*, *2*(2), 179–189. https://doi.org/10.1080/20964471.2018.1514143

Duan, A. M., Wang, M. R., Lei, Y. H., & Cui, Y. F. (2013). Trends in summer rainfall over China associated with the Tibetan Plateau sensible heat source during 1980–2008. *Journal of Climate*, *26*, 261–275. https://doi.org/10.1175/jcli-d-11-00669.1

Duan, A. M., & Wu, G. X. (2005). Role of the Tibetan Plateau thermal forcing in the summer climate patterns over subtropical Asia. *Climate Dynamics*, *24*, 793–807. https://doi.org/10.1007/s00382-004-0488-8

Ertel, H. (1942). Ein neuer hydrodynamische wirbelsatz. *Meteorologische Zeitschrift Braunschweig*, *59*, 33–49.

Flohn, H. (1957). Large-scale aspects of the "summer monsoon" in south and East Asia. *Journal of Meteorological Society of Japan*, *35A*, 180–186. https://doi.org/10.2151/jmsj1923.35a.0_180

Han, C. B., Ma, Y. M., Chen, X. L., & Su, Z. B. (2017). Trends of land surface heat fluxes on the Tibetan Plateau from 2001 to 2012. *International Journal of Climatology*, *37*, 4757–4767. https://doi.org/10.1002/joc.5119

Haynes, P. H., & McIntyre, M. E. (1987). On the evolution of vorticity and potential vorticity in the presence of diabatic heating and frictional or other forces. *Journal of the Atmospheric Sciences*, *44*, 8282–841. https://doi.org/10.1175/1520-0469(1987)044<0828:oteova>2.0.co;2

Haynes, P. H., & McIntyre, M. E. (1990). On the conservation and impermeability theorems for potential vorticity. *Journal of the Atmospheric Sciences*, *47*, 2021–2031. https://doi.org/10.1175/1520-0469(1990)047<2021:otcait>2.0.co;2

He, B. (2017). Influences of elevated heating effect by the Himalaya on the changes in Asian summer monsoon. *Theoretical and Applied Climatology*, *128*, 905–917. https://doi.org/10.1007/s00704-016-1746-5

He, B., Liu, Y. M., Wu, G. X., Wang, Z. Q., & Bao, Q. (2019). The role of air-sea interactions in regulating the thermal effect of the Tibetan-Iranian Plateau on the Asian summer monsoon. *Climate Dynamics*, *52*, 4227–4245. https://doi.org/10.1007/s00382-018-4377-y

He, B., Wu, G. X., Liu, Y. M., & Bao, Q. (2015). Astronomical and hydrological perspective of mountain impacts on the Asian summer monsoon. *Scientific Reports*, *5*. https://doi.org/10.1038/srep17586

Held, I. M. (1983). Stationary and quasi-stationary eddies in the extratropical troposphere. In *Large-scale dynamical processes in the atmosphere* (pp. 127–168). London: Academic Press.

Held, I. M., & Ting, M. (1990). Orographic versus thermal forcing of stationary waves: The importance of the mean low-level wind. *Journal of the Atmospheric Sciences*, *47*, 495–500. https://doi.org/10.1175/1520-0469(1990)047<0495:ovtfos>2.0.co;2

Held, I. M., Ting, M, & Wang, H. L. (2002). Northern winter stationary waves: Theory and modeling. *Journal of Climate*, *15*, 2125–2144. https://doi.org/10.1175/1520-0442(2002)015<2125:nwswta>2.0.co;2

Hersbach, H., Bell, B., Berrisford, P., Hirahara, S., Horanyi, A., Munoz-Sabater, J., et al. (2020). The ERA5 global reanalysis. *Quarterly Journal of the Royal Meteorological Society*, *146*, 1999–2049. https://doi.org/10.1002/qj.3803

Hoskins, B. J. (1991). Towards a PV-theta view of the general-circulation. *Tellus Series A: Dynamic Meteorology and Oceanography*, *43*, 27–35. https://doi.org/10.1034/j.1600-0870.1991.t01-3-00005.x

Hoskins, B. J., & Karoly, D. J. (1981). The steady linear response of a spherical atmosphere to thermal and orographic forcing. *Journal of the Atmospheric Sciences*, *38*, 1179–1196. https://doi.org/10.1175/1520-0469(1981)038<1179:tslroa>2.0.co;2

Hoskins, B. J., McIntyre, M. E., & Robertson, A. W. (1985). On the use and significance of isentropic potential vorticity maps. *Quarterly Journal of the Royal Meteorological Society*, *111*, 877–946. https://doi.org/10.1256/smsqj.47001

Hsu, H. H., & Liu, X. (2003). Relationship between the Tibetan Plateau heating and East Asian summer monsoon rainfall. *Geophysical Research Letters*, *30*, 4. https://doi.org/10.1029/2003gl017909

Liu, Y. M., Hoskins, B. J., & Blackburn, M. (2007). Impact of Tibetan orography and heating on the summer flow over Asia. *Journal of the Meteorological Society of Japan*, *85*, 1–19. https://doi.org/10.2151/jmsj.85b.1

Liu, Y. M., Lu, M. M., Yang, H. J., Duan, A. M., He, B., Yang, S., & Wu, G. X. (2020). Land-atmosphere-ocean coupling associated with the Tibetan Plateau and its climate impacts. *National Science Review*, *7*, 534–552. https://doi.org/10.1093/nsr/nwaa011

Liu, Y. M., Wang, Z. Q., Zhuo, H. F., & Wu, G. X. (2017). Two types of summertime heating over Asian large-scale orography and excitation of potential-vorticity forcing II. Sensible heating over Tibetan-Iranian Plateau. *Science China Earth Sciences*, *60*, 733–744. https://doi.org/10.1007/s11430-016-9016-3

Luo, H., & Yanai, M. (1984). The large-scale circulation and heat-sources over the Tibetan Plateau and surrounding areas during the early summer of 1979. Part II: Heat and moisture budgets. *Monthly Weather Review*, *112*, 9662–989. https://doi.org/10.1175/1520-0493(1984)112<0966:tlscah>2.0.co;2

Ma, Y., Zhong, L., Su, Z., Ishikawa, H., Menenti, M., & Koike, T. (2006). Determination of regional distributions and seasonal variations of land surface heat fluxes from landsat-7 enhanced thematic mapper data over the central Tibetan Plateau area. *Journal of Geophysical Research*, *111*. https://doi.org/10.1029/2005jd006742

Ma, Y., Zhong, L., Wang, B., Ma, W., Chen, X., & Li, M. (2011). Determination of land surface heat fluxes over heterogeneous landscape of the Tibetan Plateau by using the modis and in situ data. *Atmospheric Chemistry and Physics*, *11*, 10461–10469. https://doi.org/10.5194/acp-11-10461-2011

Molnar, P., England, P., & Martinod, J. (1993). Mantle dynamics, uplift of the Tibetan Plateau, and the Indian monsoon. *Reviews of Geophysics*, *31*, 357–396. https://doi.org/10.1029/93rg02030

Queney, P. (1948). The problem of air flow over mountains: A summary of theoretical studies. *Bulletin of the American Meteorological Society*, *29*, 16–26. https://doi.org/10.1175/1520-0477-29.1.16

Rajagopalan, B., & Molnar, P. (2013). Signatures of Tibetan Plateau heating on Indian summer monsoon rainfall variability. *Journal of Geophysical Research: Atmospheres*, *118*, 1170–1178. https://doi.org/10.1002/jgrd.50124

Rossby, C. G. (1940). Planetary flow patterns in the atmosphere. *Quarterly Journal of the Royal Meteorological Society*, *66*, 68–87.

Sheng, C., Wu, G. X., Tang, Y. Q., He, B., Xie, Y. K., Ma, T. T., et al. (2021). Characteristics of the potential vorticity and its budget in the surface layer over the Tibetan plateau. *International Journal of Climatology*, *41*, 439–455. https://doi.org/10.1002/joc.6629

Son, J.-H., Kwon, J.-I., & Heo, K. Y. (2021). Weak upstream westerly wind attracts Western North Pacific typhoon tracks to west. *Environmental Research Letters*, *16*, 124041. https://doi.org/10.1088/1748-9326/ac3aa4

Son, J.-H., Seo, K.-H., & Wang, B. (2019). Dynamical control of the Tibetan Plateau on the East Asian summer monsoon. *Geophysical Research Letters*, *46*, 7672–7679. https://doi.org/10.1029/2019GL083104

Son, J.-H., Seo, K.-H., & Wang, B. (2020). How does the Tibetan Plateau dynamically affect downstream monsoon precipitation? *Geophysical Research Letters*, *47*. https://doi.org/10.1029/2020gl090543

Thorpe, A. J. (1985). Diagnosis of balanced vortex structure using potential vorticity. *Journal of the Atmospheric Sciences*, *42*, 397–406. https://doi.org/10.1175/1520-0469(1985)042<0397:dobvsu>2.0.co;2

Wang, Z. Q., Duan, A. M., & Wu, G. X. (2014). Time-lagged impact of spring sensible heat over the Tibetan Plateau on the summer rainfall anomaly in East China: Case studies using the WRF model. *Climate Dynamics*, *42*, 2885–2898. https://doi.org/10.1007/s00382-013-1800-2

Wu, G. X., Duan, A. M., Liu, Y. M., Mao, J. Y., Ren, R. C., Bao, Q., et al. (2015). Tibetan plateau climate dynamics: Recent research progress and outlook. *National Science Review*, *2*, 100–116. https://doi.org/10.1093/nsr/nwu045

Wu, G. X., He, B., Duan, A. M., Liu, Y. M., & Yu, W. (2017). Formation and variation of the atmospheric heat source over the Tibetan Plateau and its climate effects. *Advances in Atmospheric Sciences*, *34*, 1169–1184. https://doi.org/10.1007/s00376-017-7014-5

Wu, G. X., Li, W. P., Guo, H., & Liu, H. (1997). Sensible heat driven air–pump over the Tibetan Plateau and its impacts on the Asian summer monsoon. In Ye, D. Z., et al. (Eds.), *Collections on the memory of Zhao Jiuzhang*. Beijing, China: Science Press.

Wu, G. X., Liu, Y. M., He, B., Bao, Q., Duan, A. M., & Jin, F. F. (2012). Thermal controls on the Asian summer monsoon. *Scientific Reports*, *2*, 7. https://doi.org/10.1038/srep00404

Wu, G. X., Liu, Y. M., Wang, T. M., Wan, R. J., Liu, X., Li, W. P., et al. (2007). The influence of mechanical and thermal forcing by the Tibetan Plateau on asian climate. *Journal of Hydrometeorology*, *8*, 770–789. https://doi.org/10.1175/jhm609.1

Wu, G. X., & Zhang, Y. S. (1998). Tibetan plateau forcing and the timing of the monsoon onset over South Asia and the South China Sea. *Monthly Weather Review*, *126*, 9132–927. https://doi.org/10.1175/1520-0493(1998)126<0913:tpfatt>2.0.co;2

Wu, G. X., Zhuo, H. F., Wang, Z. Q., & Liu, Y. M. (2016). Two types of summertime heating over the Asian large-scale orography and excitation of potential-vorticity forcing. Part II: Over Tibetan Plateau. *Science China Earth Sciences*, *59*, 1996–2008. https://doi.org/10.1007/s11430-016-5328-2

Yanai, M. H., Li, C. F., & Song, Z. S. (1992). Seasonal heating of the Tibetan Plateau and its effects on the evolution of the Asian summer monsoon. *Journal of the Meteorological Society of Japan*, *70*, 319–351. https://doi.org/10.2151/jmsj1965.70.1B_319

Yang, K., Qin, J., Guo, X. F., Zhou, D. G., & Ma, Y. M. (2009). Method development for estimating sensible heat flux over the Tibetan Plateau from CMA data. *Journal of Applied Meteorology and Climatology*, *48*, 2474–2486. https://doi.org/10.1175/2009jamc2167.1

Ye, D. Z., & Gao, Y. X. (1979). *The meteorology of the Qinghai–Xizang (Tibet) Plateau* (p. 278). Beijing, China: Science Press.

Ye, D. Z., Luo, S. W., & Zhu, B. Z. (1957). The wind structure and heat balance in the lower troposphere over Tibetan Plateau and its surroundings. *Acta Meteorologica Sinica*, *28*, 108–121. https://doi.org/10.11676/qxxb1957.010

Yeh, T. G. (1950). The circulation of the high troposphere over China in the winter of 1945−1946. *Tellus*, *2*, 173–183. https://doi.org/10.3402/tellusa.v2i3.8548

Zhang, H., Li, W., & Li, W. (2019). Influence of late springtime surface sensible heat flux anomalies over the Tibetan and Iranian plateaus on the location of the South Asian high in early summer. *Advances in Atmospheric Sciences*, *36*, 93–103. https://doi.org/10.1007/s00376-018-7296-2

Zhang, Y., Li, Z., & Liu, B. (2015). Interannual variability of surface sensible heating over the Tibetan plateau in boreal spring and its influence on the onset time of the Indian summer monsoon. *Chinese Journal of Atmospheric Sciences*, *39*, 1059–1072.

Zhang, Y. S., & Wu, G. X. (1999). Diagnostic investigations on the mechanism of the onset of Asian summer monsoon and abrupt seasonal transitions over the northern hemisphere Part II: The role of surface sensible heating over Tibetan Plateau and surrounding regions. *Acta Meteorologica Sinica*, *57*, 56–73. https://doi.org/10.11676/qxxb1999.005

Zhao, P., & Chen, L. X. (2000). Study on climatic features of surface turbulent heat exchange coefficients and surface thermal forces over the Qinghai-Xizang Plateau. *Acta Meteorologica Sinica*, *14*(1), 13–29.

Zhu, X. Y., Liu, Y. M., & Wu, G. X. (2012). An assessment of summer sensible heat flux on the Tibetan Plateau from eight data sets. *Science China Earth Sciences*, *55*, 779–786. https://doi.org/10.1007/s11430-012-4379-2